ISSN 1028-3358, Doklady Physics, 2007, Vol. 52, No. 3, pp. 129–133. © Pleiades Publishing, Ltd., 2007.
Original Russian Text © V.F. Kravchenko, O.V. Lazorenko, V.I. Pustovoĭt, L.F. Chernogor, 2007, published in Doklady Akademii Nauk, 2007, Vol. 413, No. 1, pp. 31–35.

PHYSICS

A New Class of Fractal Ultra-Wideband Signals

V. F. Kravchenko[a], O. V. Lazorenko[b], Academician V. I. Pustovoĭt[c], and L. F. Chernogor[b]

Received August 31, 2006

PACS numbers: 42.79.Sz, 43.60.Dh
DOI: 10.1134/S1028335807030019

INTRODUCTION

The variety of communication signals that exists nowadays makes it possible to successfully solve telecommunication, information, and other important practical problems. The requirements for the qualitative properties of the corresponding systems are continually growing. New types of signals exhibiting wider potentialities were actively searched for in [1–3]. Therefore, it seems reasonable to develop a novel class of fractal ultra-wideband (FUWB) signals possessing all the advantages of both existing ultra-wideband (UWB) signals and fractal signals.

MODELS OF FRACTAL UWB SIGNALS

We call FUWB signals those UWB signals that exhibit the self-affinity property and the fractional dimension. We now consider self-similar FUWB signals. In order to denote their dimension, we also use the Minkowski dimension d_M estimated by the boxing technology [4]. The following requirements are imposed on both the models $s(t)$ of FUWB signals and spectral-density functions $S(f)$:

(1) $\int s(t)dt = 0$ or $S(f)|_{f=0} = 0$, where τ is the duration of the signal;

(2) $s(0) = s(\tau) = 0$;

(3) $s(t)$ is continuous for $t \in R$;

(4) $d_M[s(t)] \notin Z$, where Z is the set of integers;

(5) $s(t)$ is the self-affine function for $t \in [0, \tau]$.

The models of UWB signals, which are rather successful from the practical standpoint, are described by wavelet-forming functions [5, 6], many of them being UWB signals [7]. Among them, we can list the Daubechies wavelets db2, db3, and db4; symlets sym2, sym3, and sym4; coiflet wavelet coif1; biorthogonal wavelets bior3.3 and bior3.5 (Figs. 1a–1i), etc. These FUWB models have no analytical expressions and can be constructed by numerical methods only on the basis of iterative algorithms.

ANALYTICAL MODELS

As an example, we describe three analytical models of FUWB signals. Using the Weierstrass function [3, 4]

$$\sigma(t) = \sum_{n=1}^{\infty} \alpha^n \cos(\beta^n t), \quad 0 < \alpha < 1, \quad \beta > 0, \quad \alpha\beta > 1,$$

we can construct the following model of FUWB signals:

$$FUWB_1(t) = \left(1 - \sum_{n=1}^{\infty} \alpha^n \cos(3\beta^n(2t-1))\right) \times \operatorname{sgn}(2t-1)\Theta(t),$$

$$\operatorname{sgn} t = \begin{cases} 1, & t > 0; \\ 0, & t = 0; \\ -1, & t < 0; \end{cases} \quad \Theta(t) = \eta(t) - \eta(t-1),$$

where $\eta(t)$ is the Heaviside step function. The shape of the $FUWB_1(t)$ model for different α and β is shown in Figs. 1j–1l. Here, $\alpha = d_M$, and $0 < \alpha < 1$. Using the Riemann function [3, 4]

$$W(t) = \sum_{n=1}^{\infty} n^{-2} \sin(\pi n^2 t)$$

[a] *Institute of Radio Engineering and Electronics, Russian Academy of Sciences, Building 7, ul. Mokhovaya 11, GSP-9, Moscow K-9, 125009 Russia*
[b] *Karazin Kharkov National University, Kharkov, Ukraine*
[c] *Scientific and Technological Center of Unique Instrumentation, Russian Academy of Sciences, ul. Butlerova 15, Moscow, 117342 Russia*
e-mail: kvf@pochta.ru; vponomar@maol.ru; Oleg-Lazorenko@yandex.ru; vlad_pst@yahoo.com; Leonid.F.Chernogor@univer.kharkov.ua

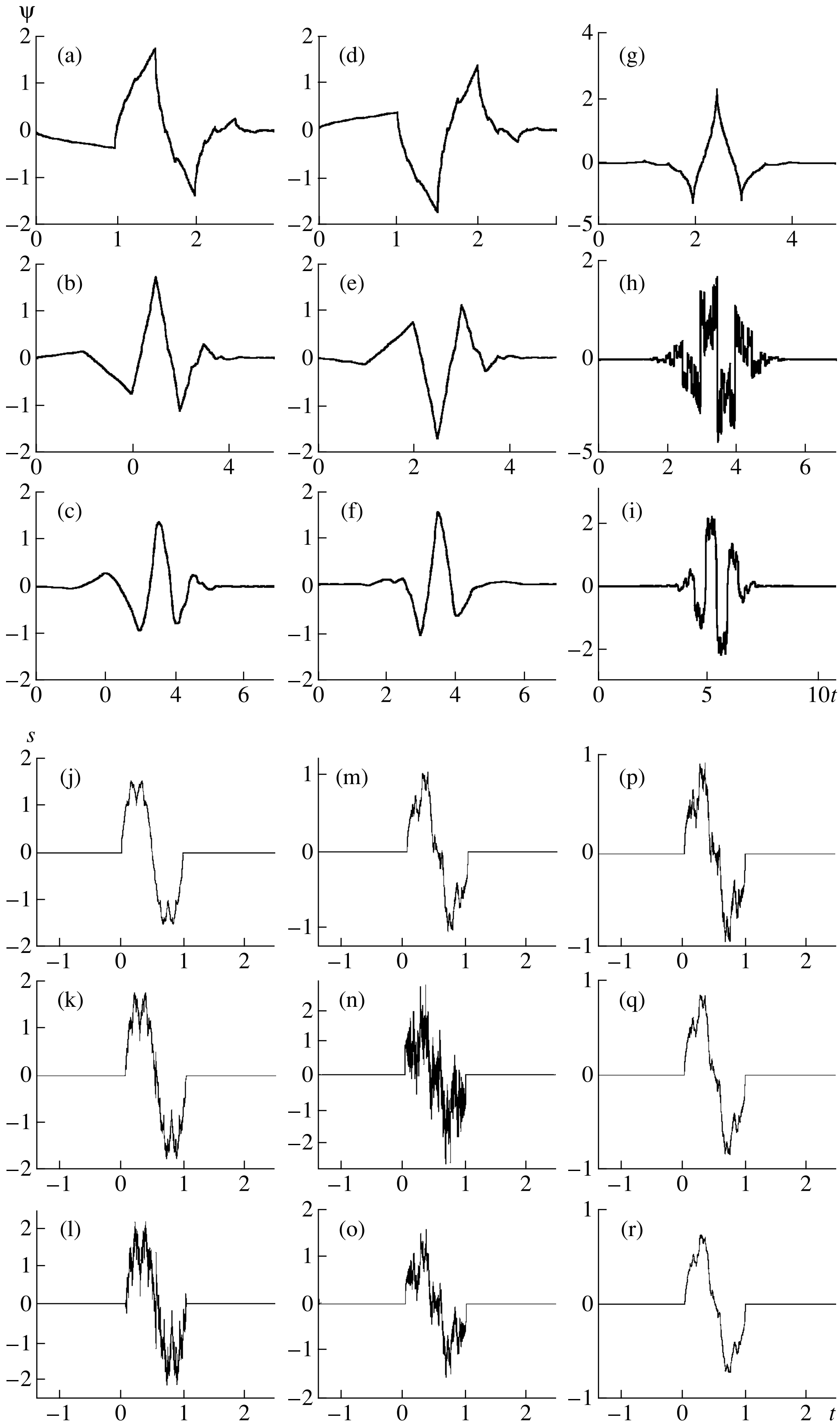

Fig. 1. Numerical and analytical models of fractal ultra-wideband (UWB) signals (wavelet-forming functions) in the time region: (a) db2; (b) db3; (c) db4; (d) sym2; (e) sym3; (f) sym4; (g) coif1; (h) bior3.3; (i) bior3.5, (j) $FUWB_1(t)$, $\alpha = 0.5$, $\beta = 2$; (k) $FUWB_1(t)$, $\alpha = 0.6$, $\beta = 2$; (l) $FUWB_1(t)$, $\alpha = 0.8$, $\beta = 2$; (m) $FUWB_2(t)$; (n) $FUWB_3(t)$, $\beta = 0.5$; (o) $FUWB_3(t)$, $\beta = 0.8$; (p) $FUWB_3(t)$, $\beta = 0.9$; (q) $FUWB_3(t)$, $\beta = 1.1$; (r) $FUWB_3(t)$.

we can also construct the model of an FUWB signal (Fig. 1m)

$$FUWB_2(t) = \sum_{n=1}^{\infty} n^{-2} \sin(2\pi n^2 t)\Theta(t).$$

The third model of an UWB signal is based on the complex-valued Riemann–Weierstrass function [3, 4]

$$W_\beta(t) = \frac{2}{\pi^\beta} \sum_{n=1}^{\infty} n^{-2\beta} \exp(i\pi n^2 t), \quad \beta > 0.5,$$

and can be written as (Fig. 1n–1r)

$$FUWB_3(t) = \frac{2}{\pi^\beta} \sum_{n=1}^{\infty} n^{-2\beta} \sin(2\pi n^2 t)\Theta(t).$$

We now compare the models for FUWB signals with one of the models for nonfractal UWB signals

$$UWB_1(t) = (-1)^n \sin(2\pi n t)\Theta(t),$$

which were proposed in [8]. Here, $N = 2n$, where N is the number of lobes for an UWB signal.

In order to describe the models of FUWB signals in the time and frequency regions, it seems to be reasonable to use the numerical characteristics described in [9] as well as the Minkowski dimension d_M.

FOURIER SPECTRUM OF AN FUWB SIGNAL

We consider the spectral-density function (SDF) of a signal in the case of the Fourier transform $S(f)$. In Fig. 2, the shapes of the functions $S(f)$ are presented for different numerical and analytical models of an FUWB signal. With increasing d_M, the side-lobe level of the SDF for a signal also rises. Nevertheless, no noticeable variations of the index μ characterizing the spectral bandwidth occur in this case. This is explained by the fact that the relative width of the SDF main maximum remains almost invariable. The matter of fact is that the values of f_{min} and f_{max} are determined according to the level of the SDF decrease by a factor of e with respect to the maximum value. At the same time, variations associated with an increase in d_M occur below this level. When the next (the second and, sometimes, the third) SDF lobes attain this level, the quantity μ exhibits a steplike change insofar as the value of f_{max} turns out not to be in the first lobe but in one of the subsequent lobes. This takes place in the case of the $FUWB_3$ and bior3.3 models for $\beta = 0.5$–0.7 (Figs. 2m and 2g, respectively). Therefore, the coefficient of the correlation between the functions μ and d_M is not high ($K \approx 0.14$). An essential negative correlation was found between the SDF width (γ_3 for the 3-dB level and d_M ($K \approx -0.17$)). This implies a disproportional distortion of the SDF main lobe, which occurs with the rise of d_M. The SDF is extended in its lower part, whereas, in contrast, the upper part is narrowed. Probably, energy transfer from the SDF main lobe to the subsequent lobes occurs. A certain dependence is observed between the relative position γ_1 of the SDF main maximum and d_M ($K \approx -0.19$). This is associated with a minor increase in the asymmetry of the SDF main lobe with the rise of d_M. The strongest correlation ($K \approx 0.46$) is observed between d_M and the equivalent signal noise band γ_8. For other numerical characteristics of an FUWB signal, a correlation dependence on d_M was not found ($|K| < 0.1$).

WAVELET SPECTRUM OF FUWB SIGNALS

The wavelet spectrum $[W_\psi s](a, b)$ of a signal is defined by both the signal model $s(t)$, in itself, and the wavelet basis used for the expansion [5]. The expression for the direct continuous wavelet transformation is of the form

$$[W_\psi s](a, b) = |a|^{-1/2} \int_{-\infty}^{\infty} s(t) \tilde{\psi}\left(\frac{t-b}{a}\right) dt,$$

where a is the scaling parameter, b is the shift parameter, and $\tilde{\psi}(t)$ is the function complex-conjugate to $\psi(t)$. A signal has a different shape in different bases. As should be expected, continuous wavelet spectra of FUWB signals are of a fractal nature. The wavelet-spectrum pattern obtained for large values of a is repeated many times for lesser values of a. As should be expected, the characteristic feature of these spectra is the presence in them spectral lines branching towards smaller values of the scaling parameter a. With the rise of d_M, this branching is enhanced. The number of branching lines increases with the number of lobes of the analyzing wavelet.

DISCUSSION OF THE RESULTS AND CONCLUSIONS

We consider the message redundancy associated with the enhanced noise immunity and also the possibility of arranging the data-transmission security as a clear advantage of FUWB signals. This is explained by the fact that the shape of many of FUWB signals (that remain strictly determinate) reminds a noiselike structure. The existence of the indicated properties of FUWB signals determines their advantage with respect to ultrashort UWB signals [10]. There is also a certain superiority of FUWB signals with respect to direct-chaotic UWB signals developed recently in [11]. The latter ones are well adapted to data-transmission security

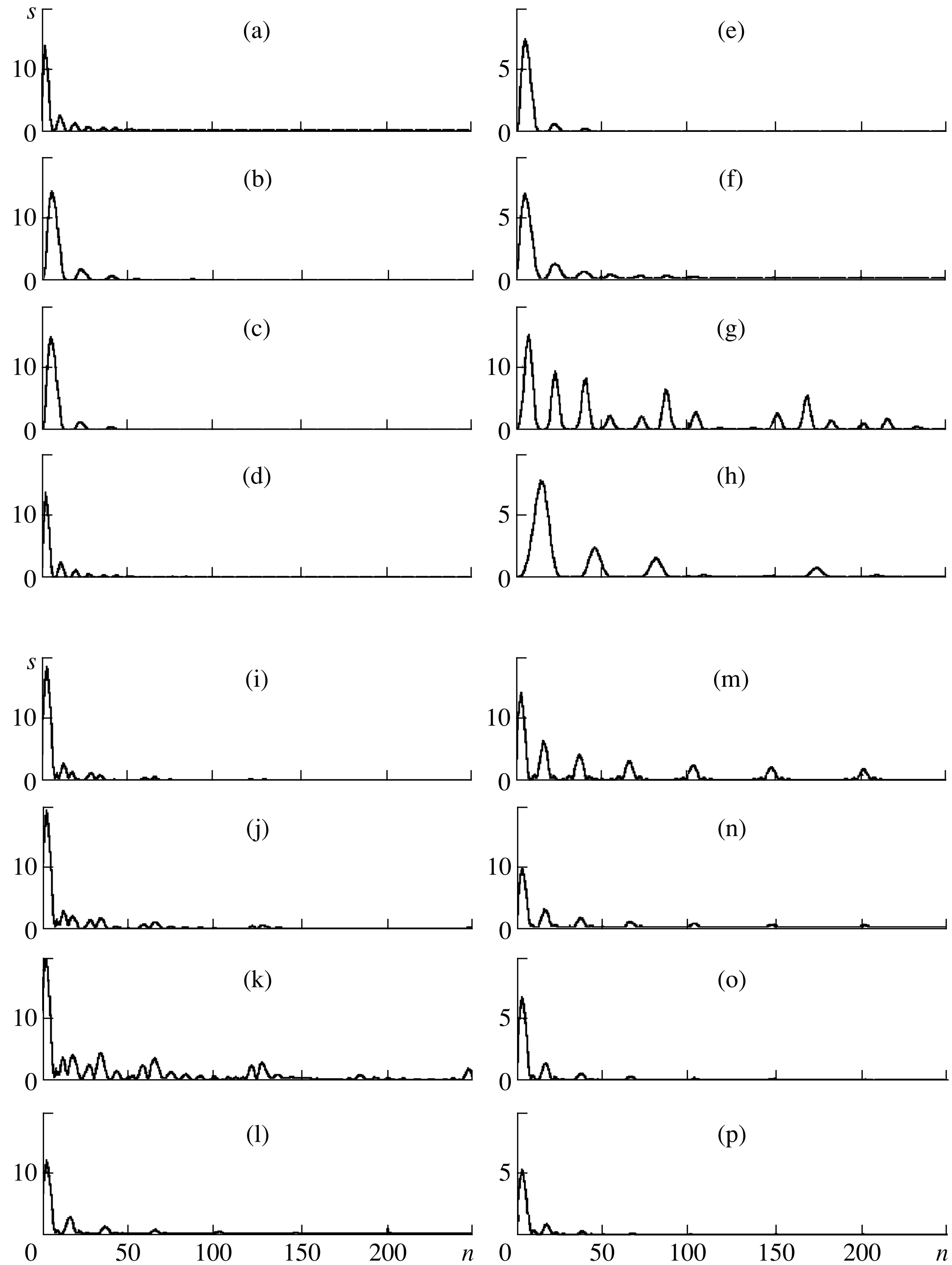

Fig. 2. Fourier spectra of numerical and analytical models for fractal ultra-wideband (FUWB) signals in the time region: (a) db2; (b) db3; (c) db4; (d) sym2; (e) sym4; (f) coif1; (g) bior3.3; (h) bior3.5; (i) $FUWB_1(t)$, $\alpha = 0.5$, $\beta = 2$; (j) $FUWB_1(t)$, $\alpha = 0.6$, $\beta = 2$; (k) $FUWB_1(t)$, $\alpha = 0.8$, $\beta = 2$; (l) $FUWB_2(t)$; (m) $FUWB_3(t)$, $\beta = 0.5$; (n) $FUWB_3(t)$, $\beta = 0.8$; (o) $FUWB_3(t)$, $\beta = 1.1$; (p) $FUWB_3(t)$, $\beta = 1.3$.

but have no fractal property and, hence, lesser noise immunity.

While using successively propagating ultrashort UWB pulses, the danger arises of the shock action of electromagnetic radiation on biological systems. Direct-chaotic UWB signals turn out to be not time structurized and not concentrated in the frequency. Therefore, their action is determined by enhancing the total background of electromagnetic radiation [11]. The FUWB signals occupy an intermediate position between these two extreme situations.

Fractal ultra-wideband signals (as well as ultrashort UWB signals) allow us to overcome difficulties associated with the problem of multibeam propagation. They can turn out to be efficient for the transmission of large (hundreds of megabytes) information arrays for distances of several kilometers. The main disadvantage of FUWB signals is associated with the necessity to develop novel methods for signal generation, emission, reception, and processing and to design the corresponding technical tools and the component basis. In addition, for FUWB signals as for UWB signals, the dispersion distortions in both the equipment and the propagation channel are strongly expressed [8].

In spite of the disadvantages indicated above, the development of the concept aimed at the use of FUWB signals seems quite reasonable insofar as the expected advantages can turn out to be rather efficient in various radiophysical applications.

REFERENCES

1. H. F. Harmuth, *Nonsinusoidal Waves for Radar and Radio Communication* (Academic, New York, 1981; Radio i Svyaz', Moscow, 1985).
2. V. F. Kravchenko, *Lectures on the Theory of Atomic Functions and Their Applications* (Radiotekhnika, Moscow, 2003) [in Russian].
3. E. G. Zelkin, V. F. Kravchenko, and V. I. Gusevskiĭ, *Constructive Approximation Methods in the Antenna's Theory* (Saĭns-Press, Moscow, 2005) [in Russian].
4. M. Holschneider, *Wavelets: An Analysis Tool* (Calderon, Oxford, 1995).
5. S. G. Mallat, *A Wavelet Tour of Signal Processing* (Academic, New York, 1998).
6. V. F. Kravchenko and V. L. Rvachev, *Boolean Algebra, Atomic Functions, and Wavelets for Application in Physics* (Fizmatlit, Moscow, 2006) [in Russian].
7. O. V. Lazorenko, S. V. Lazorenko, and L. F. Chernogor, Radiofiz. Radioastron. **7** (1), 46 (2002).
8. O. V. Lazorenko and L. F. Chernogor, Geomagn. Aeron. **37**, 747 (1997) [Geomagn. Aéron. **37** (6), 80 (1997)].
9. O. V. Lazorenko, S. V. Lazorenko, and L. F. Chernogor, Élektromagn. Volny Élektron. Sist. **9** (9/10), 31 (2004).
10. O. V. Lazorenko and L. F. Chernogor, Radiofiz. Radioastron. **10** (1), 62 (2005).
11. A. S. Dmitriev, L. V. Kuz'min, and A. I. Panas, Usp. Sovrem. Radioélektron., No. 9, 40 (2003).

Translated by G. Merzon